Enhanced Local Ternary Pattern for Texture Classification

Jing-Hua Yuan[1], Hao-Dong Zhu[2], Yong Gan[2], and Li Shang[3]

[1] College of Electronics and Information Engineering, Tongji University, Shanghai, China
[2] School of Computer and Communication Engineering,
Zhengzhou University of Light Industry, Zhengzhou, Henan, China
[3] Department of Communication Technology, College of Electronic Information Engineering,
Suzhou Vocational University, Suzhou, Jiangsu, China

Abstract. The Local Ternary Pattern (LTP) extends the conventional LBP to ternary codes and makes a significant improvement. LTP is more resistant to noise, but no longer strictly invariant to gray-level transformations. To improve the performance of LTP, this paper proposes the Enhanced Local Ternary Pattern (ELTP) by adopting the Average Local Gray Level (ALG) to take place of the traditional gray value of the center pixel, taking an auto-adaptive strategy on the selection of the threshold and introducing a novel coding process. Finally, the Completed Enhanced Ternary Pattern (CELTP) is also presented.

Keywords: Local Binary Pattern (LBP), Local Ternary Pattern (LTP), Enhanced Local Ternary Pattern (ELTP).

1 Introduction

In [1], Ojala *et al*. proposed the Local Binary Pattern (LBP) to address rotation invariant texture classification. LBP is efficient to represent local texture and invariant to monotonic gray scale transformations. Heikkila *et al*. [2] presented center-symmetric LBP (CS-LBP) by comparing center-symmetric pairs of pixels. Liao *et al*. [3] proposed Dominant LBP (DLBP) for texture classification. Tan and Triggs [4] presented Local Ternary Pattern (LTP), extending the conventional LBP to 3-valued codes. However LTP is no longer strictly invariant to gray-level transformations due to the simple strategy on the selection of the threshold. Zhang *et al*. [5] proposed Local Derivative Pattern (LDP) to capture more detailed information by introducing high order derivatives. However, if the order is greater than three, LDP is more sensitive to noise than LBP. Guo *et al*. [6] proposed Completed LBP (CLBP) by combining the original LBP with the measures of local intensity difference and central pixel gray level. Zhao *et al*. [7] proposed the Local Binary Count (LBC), to address rotation invariant texture classification by totally discarding the micro-structure which is not absolutely invariant to rotation under the huge illumination changes. However, LBC (or LBP) is sensitive to random noise and quantization noise in the near-uniform regions, as the

D.-S. Huang et al. (Eds.): ICIC 2014, LNCS 8588, pp. 443–448, 2014.

LBC (or LBP) threshold is the value of the central pixel as mentioned in [4]. Zhao *et al*. [8] presented Completed Robust Local Binary Pattern (CRLBP) by modifying the center pixel gray level to improve the LBP, but a more parameter has to be tuned.

Motivated by [4], [7], and [8],, this paper tries to address these potential difficulties by proposing the Enhanced Local Ternary Pattern (ELTP). An auto-adaptive strategy for threshold selection is adopted and a novel coding process is introduced. Furthermore, the Completed Enhanced Local Ternary Pattern (CELTP) is presented.

The remainder of this paper is organized as follows. Section **2** presents the ELTP and CELTP. Section **3** reports experimental results and Section **4** concludes the paper.

2 Enhanced Local Ternary Pattern

In order to address the demerits of LBPs, we propose Enhanced Local Ternary Pattern (ELTP). Gray-levels in a tolerance zone of width $\pm t^e$ around g_c^e are quantized to zero, ones above this are quantized to +1 and ones below it to -1, i.e., the indicator $s(x)$ used in LBP is replaced with a 3-valued function:

$$s^{\mathrm{e}}\left(g_p, g_c^{\mathrm{e}}, t^{\mathrm{e}}\right)=\begin{cases}1, & g_p - g_c^{\mathrm{e}} \geq t^{\mathrm{e}} \\ 0, & \left|g_p - g_c^{\mathrm{e}}\right| < t^{\mathrm{e}}, \quad p=0,1,...,P-1 \\ -1, & g_p - g_c^{\mathrm{e}} \leq -t^{\mathrm{e}}\end{cases} \tag{1}$$

$$g_c^{\mathrm{e}} = mean(G), \quad t^{\mathrm{e}} = mad(G), \quad G=\{g_i \mid i=0,1,...,8\}$$

where P is the size of the neighbor set of pixels, g_p (p=0, 1,..., P-1) denotes the gray value of the neighbor, G is the set of the gray-level values in a 3×3 local region, $mean(G)$ is the mean of the set G, $mad(G)$ is the median absolute deviation of the set G.

g_c is replaced by g_c^e, which make the ELTP more robust to noise. On the other hand, instead of using the simple user-specified threshold, we adopt new strategy to set the threshold t^e. To make the selection of threshold auto-adaptive, the threshold is set as the median absolute deviation (MAD), which not only reflect derivation of the local region but make the ELTP code invariant to gray-level transformations and insensitive to noise. In addition, the use of MAD does not affect the complexity of the model.

For simplicity, the experiments use a coding scheme that splits each ternary pattern into its positive half (ELTP_P) and negative half (ELTP_N) as illustrated in **Fig. 1**, subsequently combining these two separate channels of LBC descriptors to form the final ELTP descriptor and finally computing the histogram and similarity metric. Obviously, ELTP is also rotation invariant. Using the same notations as in (1), the ELTP descriptor used in the experiment is defined as follows:

$$\mathrm{ELTP}_{P,R} = \mathrm{ELTP\_P}_{P,R} * (P+2) - (\mathrm{ELTP\_P}_{P,R} * (\mathrm{ELTP\_P}_{P,R}+1))/2 + \mathrm{ELTP\_N}_{P,R}$$

$$\mathrm{ELTP\_P}_{P,R} = \sum_{p=0}^{P-1} e(s^{\mathrm{e}}\left(g_p, g_c^{\mathrm{e}}, t^{\mathrm{e}}\right), 1), \quad \mathrm{ELTP\_N}_{P,R} = \sum_{p=0}^{P-1} e(s^{\mathrm{e}}\left(g_p, g_c^{\mathrm{e}}, t^{\mathrm{e}}\right), -1), \quad e(x,y)=\begin{cases}1, & x=y \\ 0, & x\neq y\end{cases} \tag{2}$$

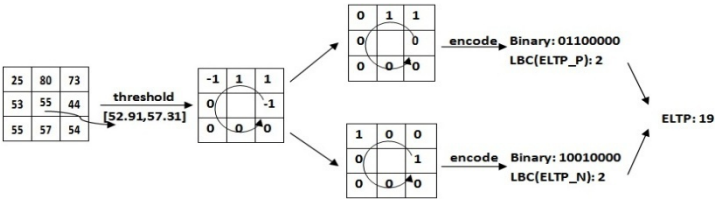

Fig. 1. The process of forming the ELTP code

Aiming to improve the discriminative capability of the local structure, the enhanced image local differences d_p^e are decomposed into two complementary components [6], i.e., the signs (s_p^e) and the magnitudes (m_p^e), respectively

$$d_p^e = s_p^e * m_p^e, \quad s_p^e = s^e\left(g_p, g_c^e, t^e\right), \quad m_p^e = ((g_p - g_c^e) - s_p^e * t^e) * s_p^e,\ p = 0, 1, ..., P. \quad (3)$$

Similar to the CLBP, we also proposed Completed Enhanced Local Ternary Pattern (CELTP) which contain three operators: CELTP_S, CELTP_M and CELTP_C. Generally, the CELTP_S equals to the original ELTP described above. And the CELTP_M and CELTP_C can be defined as:

$$\begin{aligned}
&\mathrm{CELTP_M}_{P,R} = \mathrm{CELTP_MP}_{P,R} * (P+2) - (\mathrm{CELTP_MP}_{P,R} * (\mathrm{CELTP_MP}_{P,R} + 1))/2 + \mathrm{CELTP_MN}_{P,R} \\
&\mathrm{CELTP_MP}_{P,R} = \sum_{p=0}^{P-1} s(m_p^e - m_I^e) * e(s_p^e, 1), \quad \mathrm{CELTP_MN}_{P,R} = \sum_{p=0}^{P-1} s(m_p^e - m_I^e) * e(s_p^e, -1) \\
&\mathrm{CELTP_C}_{P,R} = s(g_c^e - c_I)
\end{aligned} \quad (4)$$

where the threshold m_I^e is the mean value of m_p^e of the whole image and the threshold c_I is set as the mean gray level of the whole image.

3 Experimental Results

To evaluate the proposed method, we carried out experiments on two benchmark texture databases: the Outex database [9], which includes 24 classes of textures collected under three illuminations and at nine angles, and the CUReT database [10], which contains 61 classes of real-world textures captured at different viewpoints and illumination orientations. And we assume that the nearest neighborhood classifier and the χ^2 statistics [11][12,13,14,15,16,17] are used. For two histograms, $H=\{h_i\}$ and $K=\{k_i\}$, their dissimilarity can be calculated as: $d_{\chi^2}(H,K) = \sum_{i=1}^{N} (h_i - k_i)^2 / h_i + k_i$.

Table 1. Classification Rate (%) on TC10 and TC12 Using Different Methods

	$R=1, P=8$				$R=2, P=16$				$R=3, P=24$			
	TC10	TC12		Average	TC10	TC12		Average	TC10	TC12		Average
		t184	horizon			t184	horizon			t184	horizon	
LBP [15]	84.82	65.46	63.68	71.32	89.40	82.27	75.21	82.29	95.08	85.05	80.79	86.97
LTP [15]	76.06	62.56	63.42	67.34	96.11	85.20	85.87	89.06	98.64	92.59	91.52	94.25
CLBP_M [15]	81.74	59.31	62.78	67.94	93.67	73.80	72.41	79.96	95.52	81.18	78.66	85.12
CLBP_S/M/C [15]	96.56	90.30	92.29	93.05	98.72	93.54	93.91	95.39	98.93	95.32	94.54	96.26
CLBC_S/M/C [16]	97.16	89.79	92.92	93.29	98.54	93.26	94.07	95.29	98.78	94.00	93.24	95.67
CRLBP_S/M/C(α=1) [17]	96.54	91.16	92.06	93.25	**98.85**	96.67	96.97	97.50	**99.48**	97.57	97.34	98.13
CRLBP_S/M/C(α=8) [17]	**97.55**	**91.94**	**92.45**	**93.98**	98.59	95.88	96.41	96.96	99.35	96.83	96.16	97.45
ELTP	79.06	67.82	76.34	74.41	97.14	90.95	91.00	93.03	96.54	93.96	93.22	94.57
CELTP_M	80.83	70.81	74.63	75.42	97.06	90.88	91.50	93.15	98.59	96.46	96.25	97.10
CELTP_M/C	87.99	78.31	83.17	83.16	92.27	86.92	89.58	89.59	94.51	92.08	93.54	93.38
CELTP_S_M/C	87.81	76.67	82.94	82.47	93.67	90.56	91.34	91.86	95.55	94.65	95.76	95.32
CELTP_S/C	87.58	76.64	86.32	83.51	98.18	94.93	95.76	96.29	98.46	93.63	95.72	95.94
CELTP_M_S/C	87.89	77.50	86.20	83.86	98.83	**96.71**	**97.29**	**97.61**	99.40	**98.56**	**98.61**	**98.86**
CELTP_S_M	82.68	71.25	77.94	77.29	98.39	96.00	95.97	96.79	99.40	98.45	98.08	98.64
CELTP_S_M_C	87.50	76.39	84.56	82.82	98.54	95.58	95.70	96.64	99.43	98.17	97.92	98.51

Table 2. Classification Rate (%) on CUReT Using Different Methods

	$R=1, P=8$				$R=2, P=16$				$R=3, P=24$			
	46	23	12	6	46	23	12	6	46	23	12	6
LBP [15]	80.63	74.81	67.84	58.70	86.37	81.05	74.62	66.17	86.37	81.21	74.71	66.55
LTP [15]	85.13	79.25	72.04	63.09	92.66	87.30	80.22	70.50	91.81	85.78	77.88	67.77
CLBP_M [15]	75.20	67.96	60.27	51.49	85.48	79.01	71.24	61.59	82.16	76.23	69.22	60.45
CLBP_S/M/C [15]	**95.59**	**91.35**	84.92	74.80	95.86	92.13	86.15	77.04	94.74	90.33	83.82	74.46
CLBC_S/M/C [16]	94.78	90.12	82.92	72.85	95.39	91.30	85.91	75.14	95.26	90.55	84.07	73.18
CRLBP_S/M/C (α=1) [17]	94.55	89.47	82.72	73.22	94.78	91.10	85.47	76.39	95.35	90.73	85.05	76.34
CRLBP_S/M/C (α=8) [17]	95.39	91.33	**85.40**	**76.56**	95.88	91.85	86.44	**77.79**	96.27	91.83	86.06	**78.43**
ELTP	84.98	78.73	70.85	60.57	90.00	85.20	78.01	67.90	90.45	85.70	78.92	69.28
CELTP_M	84.83	78.46	70.36	60.25	92.31	87.44	80.25	70.23	91.24	86.01	78.55	68.32
CELTP_M/C	85.62	77.23	67.15	54.77	90.47	83.59	74.68	63.40	92.48	86.84	78.72	67.75
CELTP_S_M/C	87.36	79.53	69.62	57.05	92.03	85.99	77.86	66.84	94.25	89.51	82.32	72.00
CELTP_S/C	87.36	79.70	69.98	57.70	95.02	90.85	84.49	74.67	94.95	91.14	85.02	75.58
CELTP_M_S/C	88.43	80.65	70.90	58.66	**96.46**	**92.89**	**86.97**	77.62	**96.30**	**92.68**	**86.59**	77.03
CELTP_S_M	88.89	83.06	75.09	64.79	94.50	90.21	83.59	73.84	94.66	90.34	83.67	73.79
CELTP_S_M_C	91.49	85.67	77.57	66.99	95.34	91.08	84.42	74.57	95.18	90.95	84.28	74.35

Table 1 and Table 2 list the experimental results by different schemes on the two databases, from which we could make the following findings. Firstly, on both databases, the proposed CELTP method is inferior to CLBP_S/M/C, CLBC_S/M/C and CRLBP_S/M/C on the condition (R=1, P=8) .This mainly because we use the mean of the gray-level values in a 3×3 region to replace the value of the center pixel. Secondly, on the Outex database, ELTP performs much better than LBP except for the experiment (R=1, P=8) on TC10 dataset and outperform LTP except for the experiment(R=3, P=24) on TC10 dataset LTP; on the CUReT database, ELTP outperforms LBP and achieve similar accurate classification rate compared with LTP. It should be noticed that ELTP is much more robust to viewpoint and illumination variations. Thirdly, CELTP_M achieves impressive performance as compared with CLBP_M. This means that CELTP_M could capture more discriminative gray-level information than CLBP_M. Finally, except for the experiment (R=1, P=8), CELTP_M_S/C and CELTP_S_M almost always outperform other methods on TC12 dataset and on the CUReT database, which is impressive when the feature dimensionality is concerned.

In one word, CELTP, with low feature dimensionality, achieves better results than other methods and is less sensitive to viewpoint and illumination variations.

4 Conclusion

The Enhanced Local Ternary Pattern (ELTP) is proposed by introducing an average local gray-level strategy and an auto-adaptive threshold selection scheme, which make the proposed ELTP not only resistant to noise but also strictly invariant to gray-level transformations. To use the 3-valued codes, we also gave a novel coding scheme. Finally, we proposed Completed Enhanced Local Ternary Pattern (CELTP). Experimental results obtained from two representative databases clearly demonstrate that the proposed CELTP can obtain impressive texture classification accuracy.

Acknowledgments. This work is supported by the Science and Technology Innovation Outstanding Talent Plan Project of Henan Province of China under Professor De-Shuang Huang (No.134200510025), the National Natural Science Foundation of China (Nos. 61373105, 61373098 & 61133010).

References

1. Ojala, T., Pietikainen, M., Maenpaa, T.: Multiresolution Gray-Scale And Rotation Invariant Texture Classification with Local Binary Patterns. IEEE Trans. Pattern Anal. Mach. intell. 24(7), 971–987 (2002)
2. Heikkila, M., Pietikainen, M., Schmid, C.: Description of interest Regions with Center-Symmetric Local Binary Patterns. Proc. of Computer Vision, Graphics and Image Processing 43(38), 58–69 (2006)
3. Liao, S., Law, M.W.K., Chung, A.C.S.: Dominant Local Binary Patterns for Texture Classification. IEEE Trans. Image Process. 18(5), 1107–1118 (2009)
4. Tan, X.Y., Triggs, B.: Enhanced Local Texture Feature Sets for Face Recognition Under Difficult Lighting Conditions. IEEE Trans. Image Process. 19(6), 1635–1650 (2010)
5. Zhang, B., Gao, Y., Zhao, S., Liu, J.: Local Derivative Pattern Versus Local Binary Pattern: Face Recognition with High-Order Local Pattern Descriptor. IEEE Trans. Image Process. 19(2), 533–544 (2010)
6. Guo, Z.H., Zhang, L., Zhang, D.: A Completed Modeling of Local Binary Pattern Operator for Texture Classification. IEEE Trans. Image Process. 19(6), 1657–1663 (2010)
7. Zhao, Y., Huang, D.-S., Jia, W.: Completed Local Binary Count for Rotation invariant Texture. IEEE Trans. on Image Process. 21(10), 4492–4497 (2012)
8. Zhao, Y., Jia, W., Hu, R.-X., Min, H.: Completed Robust Local Binary Pattern for Texture Classification. Neurocomputing 10(6), 68–76 (2013)
9. Ojala, T., Maenpaa, T., Pietikainen, M., Viertola, J., Kyllönen, J., Huovinen, S.: Outex - New Framework for Empirical Evaluation of Texture Analysis Algorithms. In: Proc. 16th int. Conf. Pattern Recognit., vol. 1, pp. 701–706 (2002)

10. Dana, K.J., van Ginneken, B., Nayar, S.K., Koenderink, J.J.: Reflectance and Texture of Real World Surfaces. ACM Trans. Graph. 18(1), 1–34 (1999)
11. Varma, M., Zisserman, A.: A Statistical Approach to Texture Classification from Single Images. Int. J. Comput. Vision 62(1-2), 61–81 (2005)
12. Wang, X.F., Huang, D.S., Xu, H.: An Efficient Local Chan-Vese Model for Image Segmentation. Pattern Recognition 43(3), 603–618 (2010)
13. Li, B., Huang, D.S.: Locally Linear Discriminant Embedding: An Efficient Method for Face Recognition. Pattern Recognition 41(12), 3813–3821 (2008)
14. Huang, D.S.: Radial Basis Probabilistic Neural Networks: Model and Application. Int. Journal of Pattern Recognit., and Artificial Intell. 13(7), 1083–1101 (1999)
15. Huang, D.S., Ma, S.D.: Linear And Nonlinear Feedforward Neural Network Classifiers: A Comprehensive Understanding. Journal of Intelligent Systems 9(1), 1–38 (1999)
16. Huang, D.S.: A Constructive Approach for Finding Arbitrary Roots of Polynomials by Neural Networks. IEEE Trans. on Neural Networks 15(2), 477–491 (2004)
17. Huang, D.S., Ip, H.H.S., Chi, Z.-R.: A Neural Root Finder of Polynomials Based on Root Moments. Neural Computation 16(8), 1721–1762 (2004)